The NIST/NRL Free-Electron Laser Facility

P.H. Debenham, R.L. Ayres, J.B. Broberg, R.I. Cutler, B.C. Johnson, R.G. Johnson, E.R. Lindstrom, D.L. Mohr, J.E. Rose, J.K. Whittaker, N.D. Wilkin, and M.A. Wilson

National Institute of Standards and Technology
Gaithersburg, MD 20899, USA

C.-M. Tang and P. Sprangle

Naval Research Laboratory
Washington, DC 20375, USA

S. Penner, Rockville, MD 20852, USA

ABSTRACT

A free-electron laser (FEL) user facility is being constructed at the National Institute of Standards and Technology (NIST) in collaboration with the Naval Research Laboratory. The FEL, which will be operated as an oscillator, will be driven by the electron beam of the racetrack microtron (RTM) that is nearing completion. Variation of the electron kinetic energy from 17 MeV to 185 MeV will permit the FEL wavelength to be tuned from 200 nm to 10 μm. Performance will be enhanced by the high brightness, low energy spread, and continuous-pulse nature of the RTM electron beam. We are designing a new injector to increase the peak current of the RTM. A 3.6-m undulator is under construction, and the 9-m optical cavity is under design. The FEL will emit a continuous train of 3-ps pulses at 66 MHz with an average power of 10-200 W, depending on the wavelength, and a peak power of up to several hundred kW. An experimental area is being prepared with up to five stations for research using the FEL beam. Initial operation is scheduled for 1991.

1. INTRODUCTION

We are building a free-electron laser at the National Institute of Standards and Technology (NIST) to provide a powerful, tunable source of light for research in biomedicine, materials science, physics, and chemistry.[1] The planned research facility is shown in Figure 1. In a free-electron laser (FEL), the static, sinusoidal, magnetic field of an undulator (or wiggler) causes an electron beam to follow a sinusoidal trajectory and hence emit electromagnetic radiation. Radiation with a particular wavelength, λ, remains in phase with the electrons and stimulates additional emission; i.e., the device lases. The resonant wavelength is given by the expression

$$\lambda = (\lambda_w/2\gamma^2)\cdot(1+K^2), \qquad (1)$$

where λ_w is the wavelength of the wiggler magnetic field, and γ is the electron energy in units of the electron rest energy, E_0. The wiggler parameter, K, that appears in Equation 1 is proportional to the root-mean-square (rms) magnetic field of the wiggler, B_w:

$$K = |eB_w\lambda_w/2\pi E_0|. \qquad (2)$$

Our FEL will be driven by the electron beam of the NIST/LANL racetrack microtron (RTM), a continuous-wave (cw) accelerator that is scheduled for completion in 1990. The FEL can be characterized as a high-power, tunable, picosecond, mode-locked laser. By varying the kinetic energy of the electron beam between 17 MeV (γ = 34) and 185 MeV (γ = 363), we will be able to vary λ between 200 nm and 10 μm, from Equation (1). For our wiggler, λ_w = 28 mm, and B_w can be varied between 0.23 T and 0.38 T by varying the gap. This will allow us to tune λ by ±20% without changing γ. The laser output, like the electron beam, will be a continuous train of 3-ps long pulses at a frequency of 66 MHz. The expected properties of the output radiation are given in Table 1, and the average output power is shown in Figure 2 as a function of λ.

FEL radiation will be available for research applications in the 160-m^2 FEL user area shown in Figure 1. The photon beam will be transported in vacuum from the FEL to any of up to five experimental stations in the user area. The user area will be shielded from the electron beam and inhabitable at all times. Thus experimenters will be able to make manual adjustments to experiments in progress, as well as set up experiments when the photon beam is delivered to other stations. In the remainder of this paper we discuss the physics of microtrons and the status of our FEL project.

2. MICROTRONS

Racetrack microtrons have several properties that make them excellent sources of electrons for free-electron lasers. In this section we discuss the physics of the racetrack microtron and its predecessor, the classical microtron.

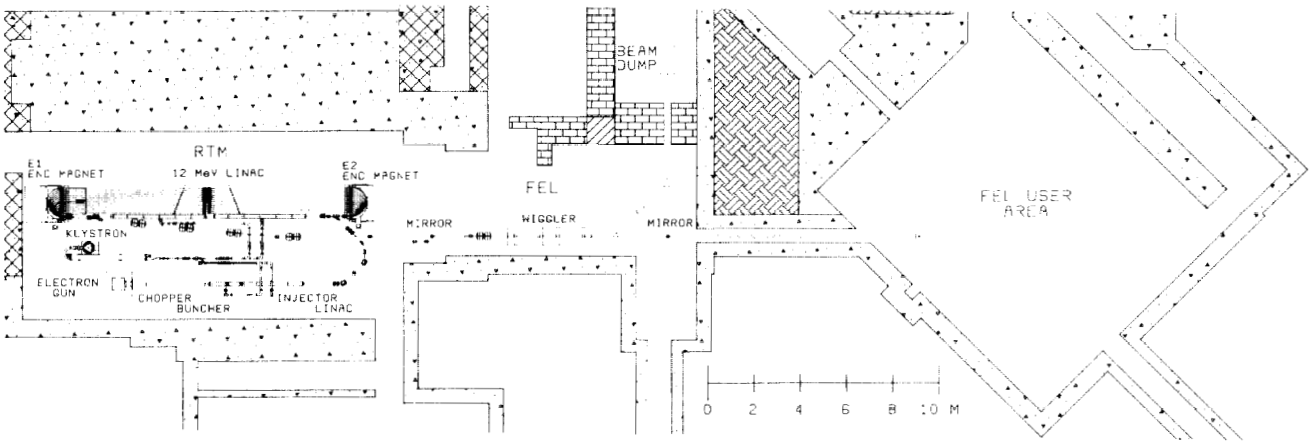

Figure 1. Plan view of the NIST/NRL FEL facility.

CH2669-0/89/0000-0775$01.00©1989 IEEE

Table 1. Output Light Properties of the NIST/NRL FEL

Wavelength	200 nm - 10 μm
Average Power (W)	10 - 200
Repetition Rate (MHz)	16.528 and 66.111
Peak Power (kW)	40 - 1000
Peak Energy (μJ)	0.1 - 3.0
Photon Flux ($cm^{-2} \cdot s^{-1}$)	10^{25} - $2 \cdot 10^{27}$
Photon Fluence (cm^{-2}, 1mm-diam spot)	$3 \cdot 10^{13}$ - $6 \cdot 10^{15}$
Pulse Width (ps)	3
Spectral Resolution	$1.4 \cdot 10^{-4}$ - $7 \cdot 10^{-3}$
Polarization	Linear
Spatial Mode	TEM_{00}
Beam Diameter (mm, at 1/e amplitude)	0.4 - 1.6
Beam Divergence (mrad, full angle)	0.3 - 5

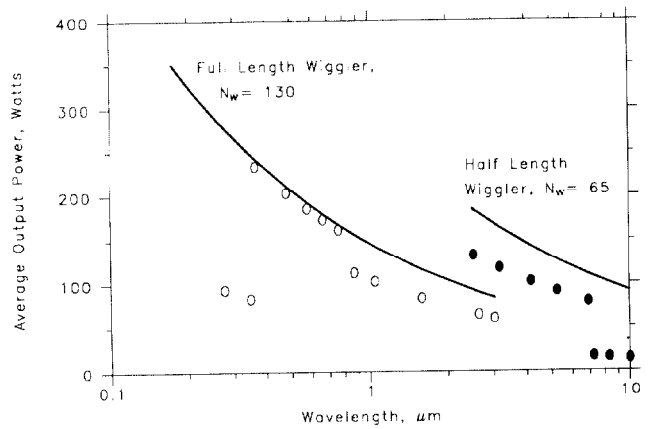

Figure 2. Predicted average output power of the NIST/NRL FEL. The solid curves show the maximum power that can be extracted from the electron beam. The circles are calculated values of output power for realistic values of mirror reflectivity and output coupling.

2.1 Classical microtron

The racetrack microtron evolved from the conventional, or classical, microtron, which was proposed by Veksler[2] in 1944. (Reference 3 provides a thorough discussion of the classical microtron.) As indicated in Figure 3, the classical microtron consists of a *microwave** cavity with an accelerating gap located in a uniform magnetic field, B. An electron that originates at one side of the gap with negligible kinetic energy crosses the gap at rf phase ϕ and in doing so gains energy $\Delta T = V \cdot \cos\phi$, where V is the peak gap voltage. The electron is returned to the gap on a circular orbit with a radius of curvature that is proportional to its momentum. The values of B and ΔT are chosen such that the circumference of the first orbit is an integral multiple of the rf wavelength, λ, and each subsequent orbit is an integral number of wavelengths, $\nu\lambda$, larger in circumference than the one before. This choice of energy gain, ΔT_r, defines a resonant phase angle, ϕ_r, such that $V \cdot \cos\phi_r = \Delta T_r$. Electrons at this phase remain in resonance with the accelerating voltage and

*Hence the name *microtron*.
†These are called end magnets.

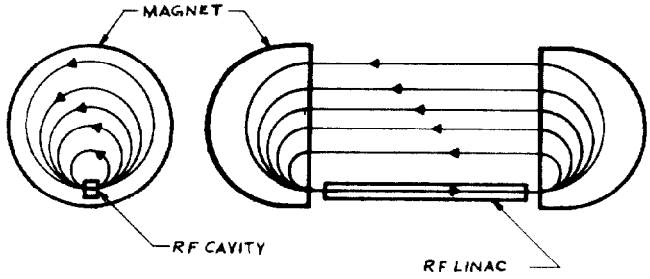

Figure 3. Classical microtron (left) and racetrack microtron.

gain energy ΔT_r each time they cross the gap. The resonant parameters are related by the microtron resonance condition,

$$2\pi \cdot \Delta T_r / c = \nu\lambda B. \qquad (3)$$

Conventional microtrons are used to produce pulsed electron beams at energies of 5 MeV to 45 MeV. The resonant energy gain per pass, ΔT_r, is limited to approximately 1 MeV. The maximum energy is limited by the need to use a relatively large, low-field magnet ($0.1\ T \leq B \leq 0.3\ T$). The microwave cavity is limited to operation in the pulsed mode by cooling limitations[4].

2.1.1 Phase focusing. Like other resonant accelerators, the microtron benefits from **phase focusing**, an important mechanism which results in good energy resolution and stability. Phase focusing comes from operating on the falling side of the microwave, so that an electron that crosses the accelerating gap before the central electron (i.e., with $\phi < \phi_r$) gains more energy than ΔT_r. The extra energy of this electron increases the length of the next orbit, and the extra distance traveled delays its next gap crossing. In this way, the phase is restored toward ϕ_r. The restoring force produces phase oscillations around ϕ_r with an amplitude equal to the initial phase spread in the electron bunch, so the phase spread remains constant as the electrons are accelerated.

Likewise, electrons that begin at the resonant phase with excess energy will arrive at the gap late the next time and gain less than ΔT_r. Thus, the initial energy spread in the beam is preserved.

2.2 Racetrack microtron

Reference 4 is a comprehensive study of the racetrack microtron and other recirculating electron accelerators. The racetrack microtron, shown in Figure 3, can be thought of as a classical microtron with its circular magnet separated into two semicircular ones† and its microwave cavity replaced by a multi-cavity linear accelerating structure, *viz.*, a linac. The electron orbits resemble a nested series of racetracks having a common homestretch and increasingly distant backstretches. The space between the magnets is exploited for several improvements. A linac can provide an energy gain on the order of 10 MeV and can be cooled adequately for cw operation. Focusing elements can be included on the straight sections.

Racetrack as well as conventional microtrons are governed by Equation 3 and benefit from phase focusing. From Equation 3 it can be seen that the increased ΔT_r allows the use of a higher magnetic field (approximately 1 T) and therefore smaller, more efficient magnets.

A racetrack microtron with N passes through a linac of energy gain ΔT_r can be compared with a single-pass electron linac of energy gain $N \cdot \Delta T_r$, to which we will refer as a "straight" linac. The RTM linac is shorter than the straight linac by a factor of N, which is typically between 10 and 50. This can lead to a significant reduction in the initial cost of the linac, its enclosure, and radiation shielding, which more than compensates for the cost of the end magnets and return beam lines. Moreover, the power dissipated in the shorter linac is lower by a factor of N, a saving that can make cw operation affordable. Finally, the straight linac does not provide phase focusing and consequently tends to have a larger beam energy spread and poorer energy stability than the RTM.

3. THE NIST/LANL RTM

The NIST racetrack microtron arose from the need for cw electron accelerators for nuclear physics in the late 1970's. Existing pulsed accelerators were not suitable for doing experiments in which several subatomic particles are detected coming from a nuclear reaction initiated by a single electron. High event rates during the pulse increase the probability of detecting unrelated but coincident particles from separate reactions to the point where the signal from true coincidences is obscured. One solution to this problem is to reduce the peak electron current without reducing the average current (hence the true event rate) by increasing the duty factor of the accelerator.

Existing US cw electron accelerators based on cryogenic, superconducting linacs[5] were limited in average current by the phenomenon of beam breakup, or BBU†. Encouraged by the successful RTM at Mainz[6], we began in 1980 the construction of a high-current, 185-MeV, cw RTM with a room-temperature linac at NIST. This was a joint project with Los Alamos National Laboratory (LANL), funded by the US Department of Energy (DoE), to determine the feasibility of a 1 to 2 GeV, cw, high-current, room-temperature, recirculating electron accelerator for nuclear physics. The design of the NIST/LANL RTM was thus strongly influenced by requirements for a 1 to 2 GeV accelerator. For example, the product of the number of passes (N) and the average beam current ($\bar{I}$) is the same in the two machines, close to the threshold for beam breakup.

†BBU is self-destructive deflection of the beam by unwanted modes of the accelerating structure that are excited by the beam. Superconducting, low-loss structures are especially vulnerable to BBU because the unwanted modes can be excited by relatively low-current beams.

When the DoE project ended in 1987, we realized that the RTM would make an excellent FEL driver and began the present project.

3.1 Design

The NIST/LANL RTM is described in Reference 7. Table 2 gives the design parameters of the accelerator and some measured beam properties. Shown in Figure 4, the accelerator comprises a 5-MeV injector connected to

Table 2. NIST/LANL RTM Parameters

	Original Design	Observed as of 3/89	Modified Design for FEL
Injection energy (MeV)	5	5.5	5
Energy gain per pass (MeV)	12	11.2	12
Number of passes	1-15	1	1-15
Output energy (MeV)	17-185	16.2	17-185
Average current (μA)	10-550	630	10-550
Accelerating frequency (MHz)	2380	2380	2380
End magnet field (T)	1.0	1.0	1.0
Peak current (A)	≤0.066	-	2-4
Micropulse length (ps)	3.5	-	3.5
Micropulse frequency (MHz)	2380	2380	66.111 16.528
Macroscopic duty factor	1.0	1.0	1.0
Energy spread (keV)	≤40	18	≤40
Normalized emittance* (μm)	≤10	2.4	≤10

*In the two-dimensional phase space of beam size and beam divergence, the emittance, ε, is the area which contains 95% of the beam, divided by π. Normalized emittance = βγε, where β is the electron velocity divided by c.

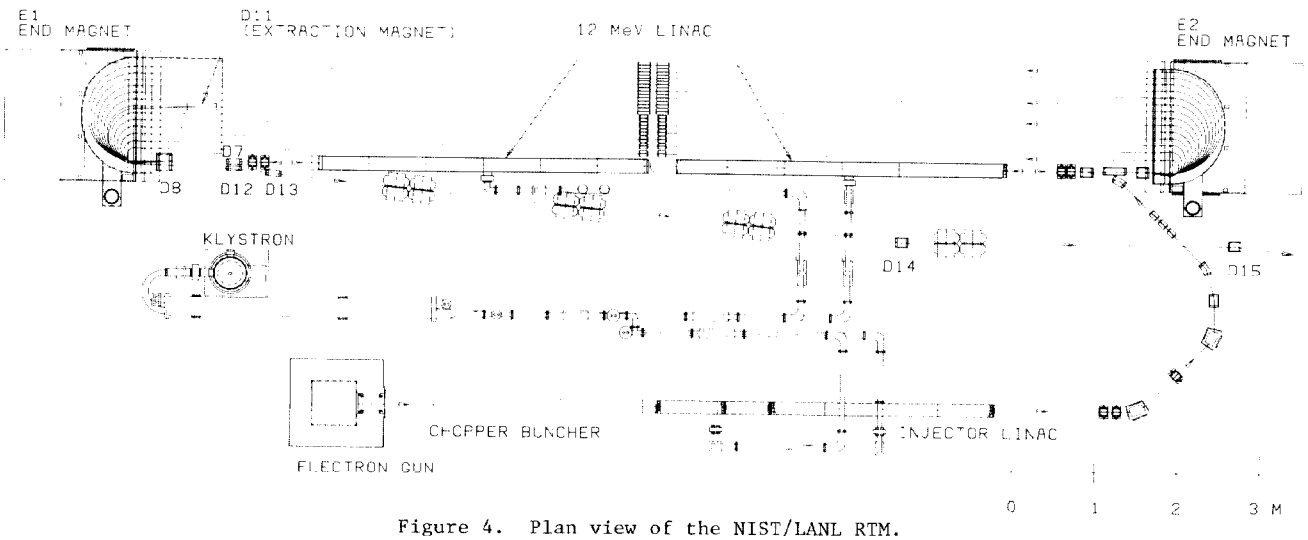

Figure 4. Plan view of the NIST/LANL RTM.

a racetrack microtron by a 180-degree beam transport system. With a floor area of 5 m by 16 m, the RTM is compact for a 185-MeV, cw accelerator. The average beam power at full energy is 100 kW.

The injector consists of a 100-keV, dc electron gun followed by a transverse-emittance-defining system, a chopping and bunching stage, and a 5-MeV, cw linac. In the microtron, 5-MeV electrons from the injector are recirculated for up to 15 passes through an 8-m long, 12-MeV, cw linac for a total energy gain of up to 180 MeV. The first pass is from right to left in Figure 4, following which the 17-MeV beam is given a parallel displacement by dipole magnets D7 and D8, deflected counter-clockwise through 180 degrees by end magnet E1, and returned to the linac axis by D8 and D7. With the length of the 17-MeV orbit adjusted to a half-integral multiple of λ, the 17-MeV beam enters the left end of the standing-wave linac with a 180-degree phase shift and is accelerated to the right. From this point on the beam circulates counter-clockwise through the microtron. Quadrupole magnet doublets are located at the middle of each beam-return line to provide adjustable focussing.

Beam can be extracted from the RTM after any number of passes simply by moving extraction magnet D11 to the appropriate beam-return line. The magnet deflects the beam inward, causing it to emerge from end magnet E1 outside the racetrack orbit. It is then removed from the accelerator by dipole D12 and the ensuing beam line. In this fashion the energy can be varied in steps of 12 MeV by changing nothing in the accelerator but the position and field strength of magnet D11*. Continuous energy variation is achieved by changing ΔT_r and B.

Microwave power from a single, 450-kW-output cw klystron is delivered to the injector linac and the RTM linac through a waveguide distribution system that can be seen in Figure 4. With a dissipation of approximately 50 kW in the distribution system, 100 kW in the injector linac and 200 kW in the 12-MeV linac, there is 100 kW available to accelerate the beam. Overall, the accelerator uses 1.1 MW, of which 9% is converted into beam power. By contrast, an equivalent 185-MeV linac would be 124 m long, dissipate 3.1 MW, and consume roughly 8.8 MW for the same beam power. The power saved by recirculating the beam through a relatively short linac makes cw operation feasible.

3.2 High-Current Injector

The injector produces beam pulses at the accelerating frequency, f_0, of 2380 MHz with a maximum of 0.35 pC per pulse. A peak beam current of 2-4 A is necessary for adequate gain in the FEL, corresponding to 7-14 pC per pulse. We must increase the peak current without increasing the average beam power, which is limited by the amount of rf power available. This will be done by reducing the beam pulse frequency to 66.111 MHz, the 36^{th} subharmonic of f_0. We plan to replace the present, 4-mA, dc, thermionic, electron gun with a 200-mA, thermionic gun pulsed at 66.111 MHz. Subharmonic chopping and bunching will be used to prepare the beam for the injector linac. The new injector, which is also designed to operate at 16.528 MHz, the 144^{th} subharmonic of f_0, is described in detail in Reference 8. Design parameters for the RTM with the new injector are given in the last column of Table 2.

3.3 Status and Plans

The present configuration of the RTM is with a single temporary beam line in place of the 14 beam-return lines in order to study performance with one pass through the 12 MeV linac for a nominal beam energy of 17 MeV. The beam line contains three beam profile monitors (wirescanners[9]) spaced three meters apart. After one pass, the beam is deflected clockwise by end magnet E1 through 180 degrees into the beam line for energy analysis and emittance measurement. Preliminary results are given in Table 2 and in Reference 10. The full, vertical width of the beam at 20% maximum† is about 1 mm throughout the 6-m beam line. The normalized emittance in the vertical plane is less than 2.4 μm, better than the design goal of 5 μm at 17 MeV.

The observed horizontal beam width of 1.6 mm includes the dispersion of electrons with different energies by the magnet. Assuming equal horizontal and vertical emittance, the width from dispersion is 0.8 mm, corresponding to a full energy spread of 18 keV. The observed energy spread is consistent with the measured voltage stability of the linacs of 0.1%[11]. Because the microtron is phase-focused, the energy spread should not increase significantly with recirculation, so we expect to surpass the design goal of 40 keV at full energy. By comparison, the energy spread from a 185-MeV linac with similar voltage stability would be 370 keV. In view of Equation 1, the RTM-driven FEL will have much better wavelength stability than one driven by a linac.

After completion of single-pass beam tests this spring, we will install the microtron beam-return lines. Concurrently, we will install the beam transport line between the microtron and the beam stop shown in Figure 1, without the mirror chicane (dipoles D15-18, shown in Figures 4 and 5) or the following quadrupole doublet. This arrangement will be used to commission the accelerator at full energy with the present injector in 1990. Three wirescanners spaced approximately six meters apart will provide beam size measurements for determining the transverse emittance, and a wirescanner following the 45-degree bending magnet D19 (see Figure 5) will be used to measure energy spread.

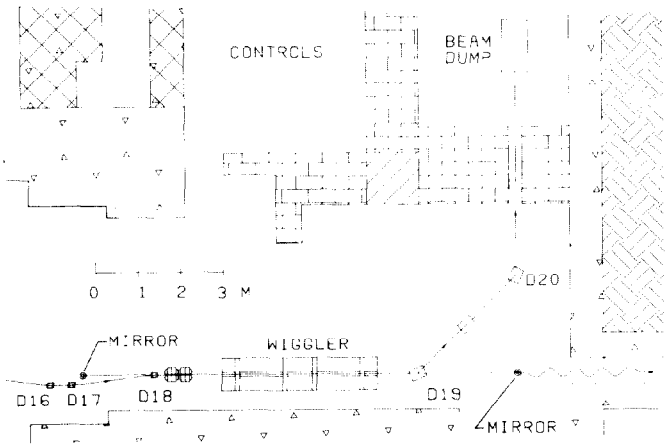

Figure 5. Plan view of the NIST/NRL FEL.

Operation of the RTM for the FEL requires a peak current of up to 40 times the original design value. The stronger wake fields that the increased peak current induces is estimated to have a non-negligible effect on beam quality. We plan to perform more detailed calculations of these effects. Operation with a decreased beam pulse frequency for the FEL could reduce the threshold current for beam breakup, I_s. This is because the accelerating structure may support BBU modes that are resonant with harmonics of the lower frequency that are not harmonics of the higher

*Of course, the magnetic fields in the beam transport line must be changed with the beam energy.

†This includes about 95% of the beam.

frequency. Preliminary calculations indicate that operation at 66.111 MHz will reduce $N \cdot I_s$ from approximately 9 mA (average) to approximately 6 mA[12]. More accurate calculations are underway. Small adjustments in focusing can produce large improvements in I_s. We are developing the high-current injector for installation in 1990, after the RTM is commissioned with the present injector. We plan to commission the new injector in 1991.

4. THE NIST/NRL FEL

4.1 Electron-beam transport

The planned electron-beam transport line from the RTM to the FEL is shown in Figures 1, 4, and 5. Following extraction from the RTM, the beam will be deflected onto the wiggler axis by dipole D14 without dispersion, i.e., with no correlation between electron energy and position or angle. Dipole magnets D15 through D18 will form an achromatic chicane to guide the beam around the upstream mirror of the FEL optical cavity and back onto the wiggler axis without dispersion.

The vertical aperture of the wiggler vacuum chamber will be 8.4 mm. The length of the wiggler will be 3.64 m for optical wavelengths between 200 nm and 2 μm. For wavelengths between 2 μm and 10 μm, we will use only the first 1.82 m of the wiggler to reduce diffraction losses. In both cases we will put the waist of the optical beam at the active center of the wiggler. The size of the waist will depend on λ. The Rayleigh length* will be half the active wiggler length to optimize transmission through the wiggler vacuum chamber. To optimize coupling between the electron and optical beams, we will use the two quadrupole magnet doublets on the wiggler axis to match the size and location of the electron-beam waist to those of the optical beam.

The spent electron beam will be removed from the FEL after the wiggler by an achromatic, 90-degree deflection system consisting of two 45-degree dipole magnets, D19 and D20, and an intermediate quadrupole magnet. The deflection system will focus the beam into a shielded beam dump behind a thick shielding wall. The energy distribution in the spent beam is an important diagnostic for lasing. This information will be obtained from a beam profile monitor located between the 45-degree magnets, where the beam will be dispersed.

4.2 Optical cavity design

The FEL optical cavity, shown in Figure 5, consists of an upstream mirror, the wiggler, and a downstream mirror. We will use a partially-transmissive downstream mirror to extract a small fraction of the optical beam from the cavity. The extracted light will be transported in vacuum to the user area. We have chosen the cavity length to be 9.070 m, twice the distance between electron pulses at 66.111 MHz, so four independent light pulses will build up in the cavity in synchronism with the electron pulses. Because the electron pulse train is continuous, the light pulses will persist in the cavity indefinitely. This eliminates the start-up problems of a pulsed FEL. For the most stable optical output, we will operate at 16.528 MHz to form a single light pulse in the cavity. Approximately four meters of electron-free length will be available for optical devices in the cavity.

ACKNOWLEDGMENTS: This work was supported in part by the US Strategic Defense Initiative Organization through ONR Contract No. N00014-87-F-0066.

4.3 Status and Plans

We have a contract with a vendor to design, construct, install and test the wiggler, including vacuum chambers, supports, controls, and a magnetic-field-mapping apparatus. The design is complete, and the main structure has been constructed. The vendor built a full-scale model of one period of the magnetic structure and performed magnetic field measurements on it to verify the design. The measured field met or exceeded all specifications. Installation of the completed wiggler at NIST is scheduled for the end of this year.

Operation of the FEL is scheduled to begin in 1991. Initially, we plan to operate at visible wavelengths, where good optical components are available. Damage to the cavity mirrors from the relatively high intracavity power is a potential problem. Multi-layer dielectric mirror coatings are available for visible wavelengths that can withstand the irradiance and fluence expected in the cavity. The absorption of these coatings is initially about 10 ppm, but is expected to increase with exposure to harmonic radiation in the FEL. While our situation is somewhat unique, experience at the LURE/ACO FEL[13] suggests that increased absorption will result in mirror failure after several days of lasing.

5. REFERENCES

1. S. Penner et al, Nucl. Inst. and Meth. in Phys. Res. A272 (1988) 73.

2. V.I. Veksler, Proc. USSR Acad. Sci. 43 (1944) 346 and J. Phys. USSR 9, (1945) 153.

3. S.P. Kapitza and V.N. Melekhin, The Microtron, Harwood, London (1978).

4. R.E. Rand, Recirculating Electron Accelerators, Harwood, London (1984).

5. P. Axel *et al.*, IEEE Trans. Nucl. Sci. NS-24 (1977) 1133.

   C.M. Lyneis, IEEE Trans. Nucl. Sci. NS-26 (1979) 3246.

6. H. Aufhaus *et al.*, Proc. of the 1981 Linear Accelerator Conference LA-9234-C (1981) 22.

7. S. Penner *et al.*, IEEE Trans. Nucl. Sci. NS-32 (1985) 2669.

8. R.I. Cutler *et al.*, "Conceptual Design of a High-Current Injector for the NIST-NRL Free-Electron Laser," to be published in Proceedings of the 1989 Particle Accelerator Conference.

9. R.I. Cutler *et al.*, Proc. 1987 IEEE Particle Accelerator Conference (1987) 625.

10. M.A. Wilson *et al.*, "NIST-Los Alamos Racetrack Microtron Status," to be published in the Proceedings of the 1988 Linear Accelerator Conference.

11. R.I. Cutler and L.M. Young, "Performance of the High-Power RF System for the NIST-Los Alamos Racetrack Microtron," to be published in the Proceedings of the 1988 Linear Accelerator Conference.

12. S. Penner, "BBU in Microtrons with Subharmonic Injection," to be published in Transactions of the 1989 IEEE Particle Accelerator Conference.

13. M. Billardon *et al.*, J. de Physique C1 (1983) 29.

*The distance from the waist to the point where the cross section of the optical beam doubles.